Inhibiting DPP4 activity protects hiPSC-derived steatotic HLCs by supporting fatty acid and purine metabolism and dampening inflammation

Christiane Loerch[1], Wasco Wruck[1], Julian, Reiss[1], James Adjaye[1,2], Nina Graffmann[1]

[1]Institute for Stem Cell Research and Regenerative Medicine, Medical Faculty and University Hospital Düsseldorf, Heinrich Heine University, Düsseldorf, Germany

[2]University College London, EGA Institute for Women`s Health, Zayed Center for Research into Rare Diseases in Children (ZGR), London, United Kingdom

*** Correspondence:**

Dr. habil. Nina Graffmann

Institute for Stem Cell Research and Regenerative Medicine

University Hospital Düsseldorf

Gebäude 14.80

Moorenstr. 5, 40225 Düsseldorf, Germany

Telephone: 0049211 8119835, Telefax: 0049211 8117858

e-mail: nina.graffmann@med.uni-duesseldorf.de

Keywords: human induced pluripotent stem cells, Hepatocyte-like cells, Dipeptidyl peptidase 4 (DPP4), Cluster of Differentiation 26 (CD26), MAFLD, MASLD, NAFLD, Steatosis, Diabetes, Vildagliptin

Number of figures and tables: 6 figures, 1 table

Conflict of interest:

The authors declare that the research was conducted in the absence of any commercial or financial relationships that could be construed as a potential conflict of interest.

Financial support:

C.L., N.G. and J.R. are funded by the Else Kröner-Fresenius-Stiftung – 2020_EKEA.64. J.A. acknowledges the medical faculty of Heinrich-Heine University Düsseldorf for part funding of this project

Authors contribution:

CL: Conceptualization, Data curation, Investigation, Methodology, Visualization, Writing–original draft, Writing–review and editing. WW: Data curation, Visualization, Writing–original draft, Writing–review and editing JR: Investigation, Methodology, JA: Conceptualization, Project administration, Resources, Supervision, Writing–original draft, Writing–review and editing. NG: Conceptualization, Formal Analysis, Funding acquisition, Investigation, Methodology, Project administration, Resources, Supervision, Visualization, Writing–original draft, Writing–review and editing

Abstract

Background and Aim: Metabolic dysfunction-associated steatotic liver disease (MASLD/MAFLD) has a high prevalence and high co-morbidity for other diseases. Due to the complexity of this multifactorial disease, therapy options are still rather limited. We employed an *in vitro* pluripotent stem cell-based model to decipher basic disease-associated molecular pathways and to study the mode of action of potential drugs.

Methods: We induced the steatosis phenotype in human induced pluripotent stem cell (iPSC) derived hepatocyte-like cells (HLCs) by oleic acid (OA)-feeding and confirmed regulation of clinically relevant pathways by NGS-based global transcriptomic analyses. Analysis of the secretome of steatotic HLCs revealed Dipeptidyl peptidase 4 (DPP4) as a potential key mediator of the disease. To further elucidate its role in the development of MAFLD, we inhibited DPP4 activity with Vildagliptin (VILDA) and analyzed the global transcriptome changes as well as specific gene and protein expression of steatosis-associated genes with and without DPP4 inhibition.

Results: MAFLD-associated pathways such as PPAR- and TNF signaling were differentially regulated in hiPSC-derived steatotic HLCs. We found increased hepatic DPP4 activity and secretion upon OA. Fatty acid and purine metabolism and inflammation response pathways were improved upon DPP4 inhibition.

Conclusion: Our HLC-model confirmed clinically-relevant association of DPP4 with metabolism and inflammation which foster the development of MAFLD. Inhibiting DPP4 with VILDA partially relieved the steatotic phenotype.

Impact and implications:

Given the difficulties of identifying suitable anti-MAFLD drugs, novel model systems are urgently needed. Our *in vitro* HLC-model reproduced DPP4-dependent aspects of

the disease and responded positively to Vildagliptin treatment. Further elucidation of the role of DPP4 in the etiology of MAFLD is warranted.

Introduction

Steatotic liver diseases are an increasing health burden for industrialized countries all over the globe(1-4). Early, reversible stages involve steatosis and steatohepatitis, resulting in fibrosis, while nascent cirrhosis and hepatocellular carcinoma are non-reversible and life-threatening. Primary causes for steatosis are elevated fatty acid flux from adipose tissue, a high-fat diet, or elevated blood glucose levels. Thus, obesity and type 2 diabetes mellitus (T2DM) are direct diagnostic criteria for Metabolic dysfunction-associated fatty/steatotic liver disease (MAFLD/MASLD)(2) . MAFLD is a complex, multisystem disease, with serious implications on the whole body, including cardiovascular disease and chronic kidney diseases(5, 6). Moreover, its multifactorial character and tissue heterogeneity is not only found in the clinic but is also shown in the molecular response to steatosis(7-9). These factors complicate research and to date resmetirom is the only FDA approved drug for treating MASLD(6, 10, 11).

Dipeptidyl peptidase 4 (DPP4) is a serine protease with catalytic activity for various substrates(12). The most prominent ones are the incretins- Glucagon like peptide 1 (GLP-1) and Glucose-dependent insulinotropic polypeptide (GIP1). However, DPP4 not only interferes with incretin signaling, but also cleaves chemotactic peptides with implications for the inflammatory response(12, 13). It is therefore considered a hepatokine, upregulated in metabolic liver disease and a driver of inflammation(13). Gliptins -potent DPP4 inhibitors- are used for the treatment of T2DM, prolonging the postprandial incretin answer(13-16). Vildagliptin (VILDA) shows additional protective effects on hepatocytes by reducing hepatic triglyceride load as well as

aminotransferase levels(17). Since the inflammatory response was reduced, it might interfere with the traits towards steatohepatitis, thus indicating a beneficial effect on the progression of the disease(18, 19).

In this study, we differentiated human patient-derived induced pluripotent stem cells (iPSCs) to hepatocyte-like cells (HLCs) by using our previously published efficient 2D differentiation protocol(20). We induced the steatosis phenotype and provide insights into the hepatocyte-specific contribution to the disease and the potential role of DPP4 for the interplay between metabolism and inflammation.

Materials and Methods

Human induced pluripotent stem cell (iPSC) culture and hepatocyte-like cell (HLC) differentiation:

The use of iPSC lines for this study was approved by the ethics committee of the medical faculty of Heinrich-Heine University under the numbers 5013 and 5704. iPSCs were cultivated on Matrigel (Corning) coated 6-well plates with daily changes of StemMACs medium (Miltenyi). Once iPSCs attained 90% confluency, they were colony-split by addition of PBS w/o magnesium or calcium (PBS-/-) (Gibco) and incubated for approximately 3 min at room temperature (RT). Colonies were detached from the surface with a cell scraper and centrifuged at 40 *xg* for 3 min. The pellet was carefully resuspended and clumps of colonies were seeded in a ratio of 1:6.

iPSCs were differentiated according to our previously published protocol(20). In brief, 1.04 x10^5 iPSCs/ cm^2 were seeded onto Matrigel-coated dishes. Definitive endoderm (DE) was induced by 1-3 days of 2.5 µM CHIR99021 (Stemgent) and 3-5 days of 100 ng/ml Activin A (Peprotech) in RPMI medium. Hepatic endoderm (HE) medium was fed for 4 days, and 1% DMSO was added with medium changes every day. HLC

medium was fed for 12-15 days, with medium changes every other day. 1 µM insulin (Sigma-Aldrich), 10 ng/mL hepatocyte growth factor (HGF) (Peprotech), 25 ng/ml dexamethasone (Dex) (Sigma-Aldrich), and 20 ng/mL recombinant human Oncostatin M (rhOSM209a.a) (Immunotools) were freshly added to the medium.

Table 1: iPSC lines used in this study.

iPSC line	Sex	Age (years)	Disease	Source	Ref.
Cntrl 1	male	50	healthy	urine derived renal progenitor cells	(21)
Cntrl 2	female	19	healthy	dermal fibroblasts	(22)
Stea 1	male	61	high grade steatosis	dermal fibroblasts	(23)
Stea 2	female	58	high grade steatosis	dermal fibroblasts	(24)

Immunocytochemistry:

Cells were washed with PBS-/-, fixed with 4% PFA for 10 min at RT, and washed 3x with PBS-/-. For intracellular staining, the cells were permeabilized with 0.5% Triton-X-100 (Sigma-Aldrich) in PBS-/- for 10 min at RT, and blocked with 3% BSA in PBS-/- for 1 h at RT. After incubation with primary antibodies (Supplementary material table S2) at respective dilutions (Table S1) overnight at 4°C, unbound antibodies were washed off 3x with PBS-/-. Secondary antibodies against the respective host IgG were incubated for 1 h at RT and washed 3x with PBS-/-. (Confocal) microscopy was performed, using a LSM 700 microscope (Zeiss) and images were processed with ZEN software (Zeiss).

Quantitative reverse transcription PCR (qRT-PCR):

RNA was isolated using the Direct-zol RNA isolation kit (Zymo Research), following the manufacturer's instructions. 500 ng of RNA was reverse transcribed to cDNA using the TaqMan reverse transcription kit (Life technologies). qRT-PCR was performed using the VIIA7 machine (Life technologies) and the power SYBR green master mix (Life technologies). Expression of mRNA was presented as log2-fold-change in comparison to the housekeeping gene and the control condition. For primer sequences please refer to the supplementary material, table S1.

Western Blot

Cells were lysed in RIPA buffer containing protease and phosphatase inhibitors (all Sigma-Aldrich). 15 - 30 µg proteins were separated on NuPAGE 4 to 12% Bis-Tris protein gels (Life Technologies) and wet-blotted onto 0.45 µm nitrocellulose membranes (Amersham). After blocking with 5% non-fat milk (ROTH) in TBS-T buffer, the membranes were incubated with the respective primary antibodies (Supplementary CTAT Table, Table S1) overnight at 4 °C. After 3x washing with TBS-T buffer, fluorescence labeled secondary antibodies (Licor) against the host IgG were incubated for 1 h at RT at a 1:10000 dilution. Unbound antibodies were washed off with TBS-T buffer and the fluorescence signal was detected at 680 nm and 800 nm by using the ChemiDoc MP Imaging system (Bio-Rad). Quantification was performed using the Image Lab 6.0.1 software with lane background subtraction using disk size 1.

Cytochrome P450 activity measurement

P450-Glo™ CYP3A4 and CYP2D6 assays (Promega) were used to measure Cytochrome P450 activity. Cells were incubated with 3 µM Luciferin-IPA or 10 µM

Luciferin-ME EGE, respectively, in William`s E Medium (Gibco) for 1 h at 37 °C. After incubation with the detection reagent, luminescence was measured in technical triplicates with a luminometer (Lumat LB 9507, Berthold Technologies).

Steatosis induction by OA-feeding and Vildagliptin (VILDA) treatment:

Oleic acid (Sigma) was bound to 14% (w/v) fatty acid free BSA (ROTH) in 0.1 M TRIS pH 8.0 for 1 h at 37 °C, and stored at 4 °C. From day 15-17 of HLC differentiation on, the cells were fed with complete HLC medium, supplemented with 400 µM OA or the respective volume of TRIS-BSA as mock-treatment. The medium was changed every other day for 7 days. A final concentration of 30µM VILDA (Sigma-Aldrich) dissolved in DMSO was fed to the cells after 48 h OA-/mock-induction for 5 days with medium changes every other day.

Next generation sequencing and analysis of deep sequencing data:

3`RNA-Seq was performed on a NextSeq2000 sequencing system (Ilumina) at the core facility Biomedizinisches Forschungszentrum Genomics and Transcriptomics laboratory (BMFZ-GTL) of Heinrich-Heine University Duesseldorf. The HISAT2 (version 2.1.0) software(25) was employed to align the fastq files received from the BMFZ-GTL core facility against the GRCh38 genome. For detailed description of the integration of the data please refer to the supplementary methods section.

GO and pathway analysis:

Subsets of genes expressed exclusively in one condition in the Venn diagram analysis and up- and down-regulated genes according to the criteria for differentially expressed genes mentioned above were subjected to over-representation analysis of gene ontologies (GOs) and KEGG (Kyoto Encyclopedia of Genes and Genomes) pathways(26). The hypergeometric test built-in in the R base package was used for over-representation analysis of KEGG pathways, which had been downloaded from the KEGG database in February 2023. The GOstats R package(27) was employed to determine over-represented GO terms. The most significant GO terms and KEGG pathways were displayed in dotplots via the R package ggplot2(28).

Enzyme-linked Immunosorbent assay (ELISA):

Secreted DPP4 was detected from supernatants 48 h after feeding using the human DPP4/CD26 DuoSet ELISA (R&D Systems) as described by the manufacturer. Optical density was measured using the EPOCH2 spectrophotometer (BioTek) at 450 nm with wavelength correction at 540 nm. 4-PL curve fitting was performed to calculate concentrations.

Enzyme activity assay:

DPP4 activity was measured in OA-/ VILDA-treated HLCs, using the Dipeptidyl peptidase IV (DPP4) Activity Assay Kit (Fluorometric)(Abcam), following the manufacturer's instructions. Fluorescence signal was measured on the EPOCH2 Spectrophotometer (BioTek) at Ex/Em = 360/460 nm.

Cytokine Array:

Supernatants of three biological replicates were harvested 24 h after medium change and Proteome Profiler Human XL Cytokine array (R&D Systems) analysis was performed following the manufacturer's protocol and signals were detected, using the Fusion FX instrument (PeqLab). Analysis and quantification was performed using the FIJI/ImageJ software(29) and the Microarray Profile plugin by Bob Dougherty and Wayne Rasband (https://www.optinav.info/MicroArray_Profile.htm, accessed on 21 December 2022). For details of the image analysis and follow-up normalization in the R/Bioconductor environment(30) we refer to the description in our previous publication(31). Cytokines were considered differentially expressed satisfying the criteria: detection p-value < 0.05 in at least one condition, fold change > 1.2 and limma-p-value < 0.05. The function heatmap.2 from the gplots package(32) and the R-builtin function barplot were applied for heatmap and bar plots.

Statistics:

Student's unpaired two-tailed t-test or ordinary one- or two-way ANOVA followed by Tukey's, Dunnet's, or Sidak's multiple comparison test were conducted to calculate significances using GraphPad Prism 8.0.2 software.

Results

iPSCs-derived hepatocyte-like cell (HLC) differentiation from four individuals

Induced pluripotent stem cells (iPSCs) derived from four individuals, two healthy controls (Cntrl 1, Cntrl 2)(21, 22) and two steatosis patients (Stea 1, Stea 2)(23,

24) (Table 1), were differentiated into HLCs following our recently published protocol(20). Representative immunocytochemistry of Cntrl 2 shows the expression of Octamer binding transcription factor 4 (OCT4) in iPSCs, SRY-box transcription factor 17 (SOX17) in definitive endoderm (DE), and Alpha-fetoprotein (AFP) in hepatic endoderm (HE) (Fig. 1A). HLCs were stained for the epithelial marker E-Cadherin (E-CAD), Hepatocyte nuclear factor 4 alpha (HNF4a) and Albumin (ALB) (Fig. 1A). Representative pictures of the other cell lines are provided in the supplementary section (Fig. S1 and S2A-C). Gene expression of HLC markers *ALB* and Cytochrome P450 family members *CYP3A4* and *CYP2D6* showed significant increases in three out of four cell lines at the HLC-stage in comparison to the iPSC-stage. Representative gene expression of *OCT4* and *SOX17* in DE, as well as *AFP* in HE stage is provided in Fig. S2D. Protein expression of AFP and ALB is shown in comparison to the housekeeping protein beta-Actin (bActin) in HLCs derived from Cntrl 1 and Cntrl 2 (Fig. 1C). HLCs' functionality was confirmed by measuring CYP3A4 and CYP2D6 activity for the four cell lines (Fig. 1D).

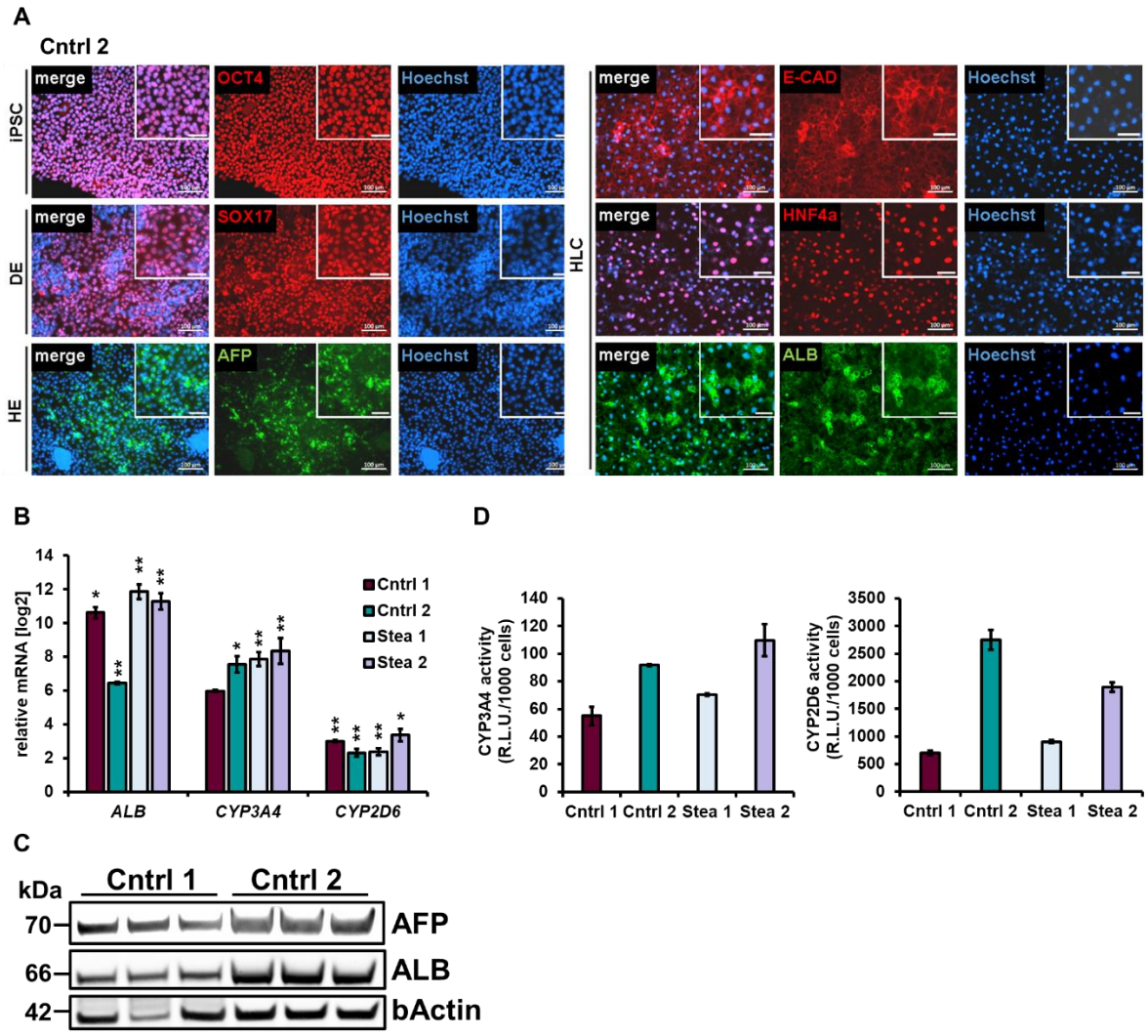

Fig. 1 Characterization of HLCs. (A) Representative immunocytochemistry of cell line Cntrl 2 during differentiation showing respective markers OCT4 in iPSCs, SOX17 in definitive endoderm (DE), and AFP in hepatic endoderm (HE). For hepatocyte-like cells (HLCs), the epithelial marker E-CAD, HNF4a and ALB are shown. Scale bars = 100 µm. **(B)** Gene expression of *ALB* and Cytochrome P450 family members *CYP3A4* and *CYP2D6* in HLCs (n=3) derived from four cell lines in comparison to iPSC-stage (n=2), shown in means of three or two biological replicates ±SE respectively, normalized to the housekeeping gene *RPLP0*. Two-tailed unpaired students' T-test was performed to calculate significances (*$p < 0.05$, **$p < 0.01$, ***$p < 0.001$). **(C)** Protein expression of AFP, ALB and bActin in HLCs derived from Cntrl 1 and Cntrl 2 (n=3). **(D)** Representative cytochrome P450 activity of HLCs is for CYP3A4 and CYP2D6 in relative light units (R.L.U.) per 1000 cells in technical triplicates (n=3).

Oleic acid (OA) induces steatosis phenotype in HLCs

To induce the steatosis phenotype in iPSC-derived HLCs, we treated HLCs of all four cell lines on day 15-17 of differentiation with 400 µM oleic acid (OA) for 7 days. After OA induction, we detected the formation of Perilipin-2 (PLIN2) coated lipid droplets by immunocytochemistry in all cell lines (Fig. 2A/B and Fig. S3). Interestingly, from a visual impression, it seemed that Cntrl 1 showed less lipid droplets than Cntrl 2, indicating a cell line specific difference in the build-up of lipid droplets. This is in line with our previous observation of differences in the size and number of LDs between different cell lines(7). To analyze the global transcriptomic changes upon OA induction, RNA-seq was performed and revealed gene expression clustering according to the treatment and based on the genetic background of each cell line (Fig. 2C). However, two samples of HLCs derived from cell line Stea 2, clustered ambiguously, (Fig. 2C, red asterisks). To prevent biases due to the genetic background of this cell line, we excluded Stea 2 in subsequent analysis. We identified 15,705 genes expressed in common in both conditions in cell lines Cntrl 1, Cntrl 2 and Stea 1, while 437 genes were exclusively expressed under OA in comparison to 393 genes solely expressed genes under mock treatment. Combining the exclusively and commonly expressed genes, we found 1,147 genes significantly upregulated and 884 genes significantly downregulated (Fig. 2D) after OA treatment. KEGG-associated pathway analysis revealed, among others, genes of the glutathione pathway and metabolic pathways significantly downregulated upon OA-treatment throughout Cntrl 1, Cntrl 2 and Stea 1 cell lines (Fig. 2E). Confirming results from a previous study(7), we found genes associated with KEGG pathways of Peroxisome proliferator activated-receptor (PPAR)-, Adenosine monophosphate-activated protein kinase (AMPK)-signaling and fatty acid metabolism significantly upregulated (Fig. 2F). Furthermore, we detected genes belonging to inflammation-related pathways significantly upregulated upon OA, such as Tumor necrosis factor (TNF) signaling and NF-kappa-B pathway. Interestingly,

also genes of the inflammatory bowel disease and insulin resistance pathways were upregulated upon OA (Fig. 2F). This KEGG-associated pathway analysis confirmed the induction of the steatosis phenotype by OA supplementation in the three cell lines Cntrl 1, Cntrl 2 and Stea 1. We performed Pearson's correlation heatmap analysis of genes associated with relevant KEGG-pathways (Fig. 3A). Notably, this revealed a change of clustering according to the treatment and independent of the genotype, indicating the relevance of these genes for the phenotype.

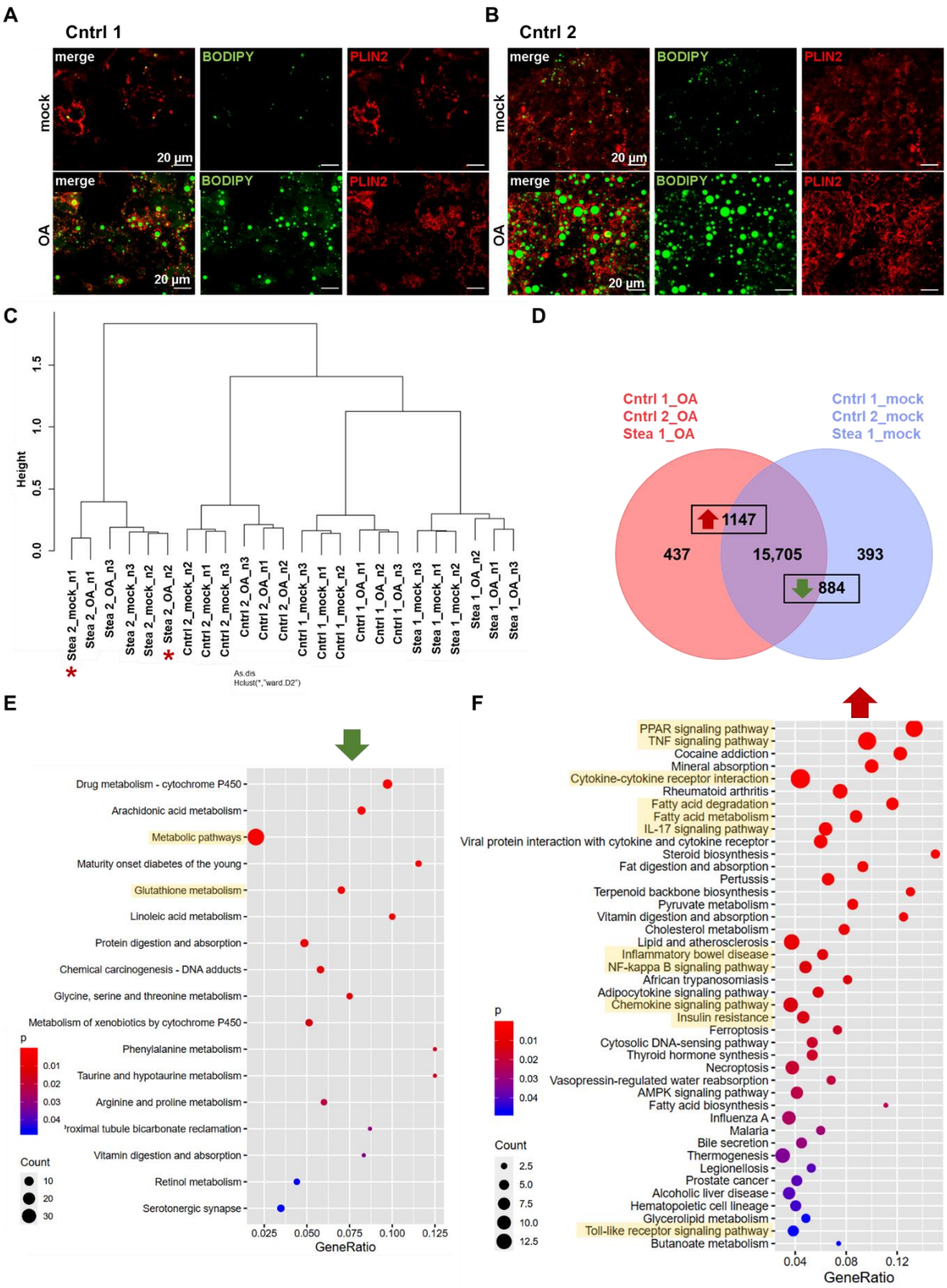

Fig. 2 Confirmation of steatosis phenotype in HLCs. (A/B) Representative immunofluorescence and BODIPY 493/503 staining of HLCs derived from Cntrl 1 and Cntrl 2 treated with 400 µM OA and respective control (mock) for 7 days PLIN2 is shown in red, fatty acids are stained in green. Scale bars represent 20 µm. **(C)** Hierarchical cluster dendrogram

of global transcriptomic changes upon OA treatment of HLCs derived from cell lines Cntrl 1, Cntrl 2, Stea 1, Stea 2 in three biological replicates (n=3). Ambiguous clustering of gene expression in Stea 2 is marked by red asterisks (Correlation in supplementary table 1). **(D)** Venn diagram of gene expression from OA treated HLCs derived from cell lines Cntrl 1, Cntrl 2, Stea 1 indicating 437 solely expressed genes upon OA, and 393 solely expressed genes upon mock treatment and 15,705 commonly detected hits. Among exclusively and commonly expressed genes 1,147 and 834 genes were significantly up- and down-regulated, respectively. **(E/F)** Dot plots of KEGG-associated pathway analysis of significantly down **(E)**- and up **(F)**-regulated genes (gene lists in supplementary table 1).

To confirm the global gene expression changes, we performed qRT-PCR for genes associated with the relevant pathways (Fig. 3B). We found significant increases of PPAR-pathway associated genes, *PLIN2* and fatty acid binding protein-1 (*FABP1)* upon OA-treatment in at least 2 out of our 3 cell lines. Regarding insulin signaling associated genes, phosphoenolpyruvate carboxykinase-1 (*PCK1*) was significantly upregulated in Cntrl 2, and a non-significant trend towards upregulation was detectable in Cntrl 1 and Stea 1. Carnitine palmitoyltransferase-1A (*CPT1A*) was significantly upregulated in Cntrl 1 and 2. Interestingly, in contrast to the RNA-seq results, we found insulin-like growth factor binding protein-1 (*IGFBP1)* to be upregulated upon OA, however not significantly. Considering genes associated with inflammation, a significant upregulation of CC-chemokine ligand 4 (*CCL4*) and interleukin 1beta (*IL1B)* expression was detected in Cntrl 1 and Stea 1, while in Cntrl 2 the increase was not - significant. We found a significant reduction in the expression of vascular cell adhesion molecule-1 (*VCAM1*) in Cntrl 2 and Stea 1. Furthermore, we found members of the renin-angiotensin-system (RAS) differentially regulated in our model. For example, Angiotensin converting enzyme 2 (*ACE2*) was upregulated in the RNA-seq data. A trend that could be confirmed by qRT-PCR. In addition, we detected a reduction of alanyl aminopeptidase (*ANPEP*), which is also involved in the glutathione metabolism

(reactive oxygen species (ROS)-regulation), in all three cell lines, albeit only significantly in Stea 1. Together, these findings strengthen the validity of our model, because clinically relevant pathways were differentially regulated upon OA. They further underline the importance of the investigated genes as their differential expression was independent of the genetic background.

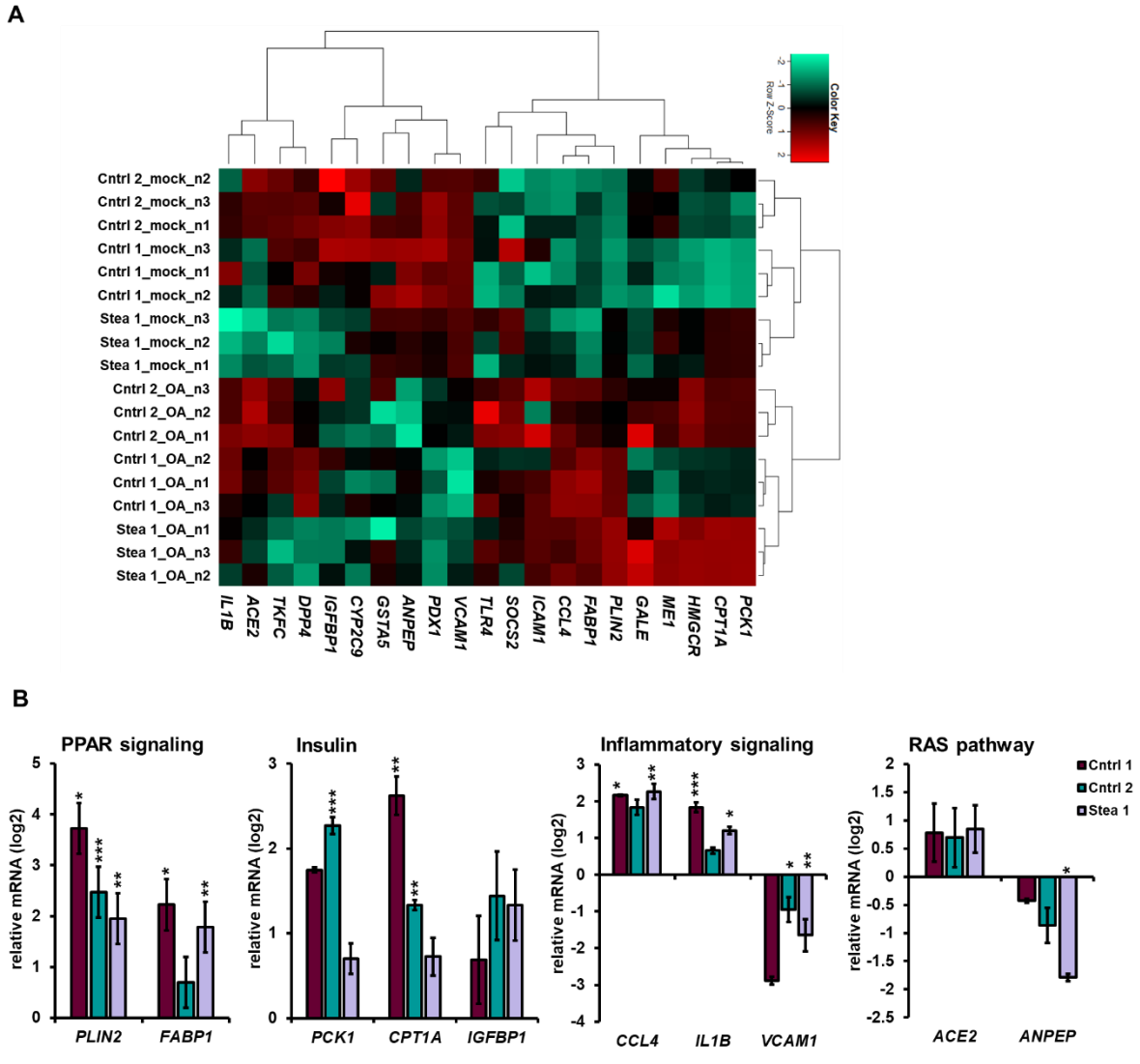

Fig. 3 OA-treatment induces differential gene expression. (A) Pearson's correlation heatmap analysis of the gene expression of members of OA-dysregulated pathways like fatty acid metabolism (*PLIN2*, *FABP1*), metabolic pathways/ glutathione metabolism (*ANPEP, GSTA5*) and insulin resistance (*PCK1*, *CPT1A*, *IGFBP1*, *SERPINA7*, *PDX1*). **(B)** qRT-PCR analysis of the mRNA expression of *PLIN2*, *FABP1, PCK1*, *CPT1A*, *IGFBP1*, *CCL4*, *IL1B, VCAM1 ACE2*, and *ANPEP* relative to mock-treated HLCs from cell lines Cntrl 1, Cntrl 2 and Stea 1 normalized to mock-treated HLCs derived from each cell line as means of two or three

biological replicates ± SE (n=2 or n=3), normalized to the housekeeping gene *RPLP0*. Two-tailed unpaired Student`s T-test was performed to calculate significances (*p < 0.05, **p < 0.01, ***p < 0.001).

Dipeptidyl peptidase 4 (DPP4) is secreted upon OA treatment

We analyzed the supernatant of OA-treated HLCs for released signaling proteins. Among others, we found a significant increase of DPP4, also known as Cluster of Differentiation 26 (CD26), upon OA-induction (Supp Fig. S4B/C). This significant increase was confirmed by ELISA for three out of four cell lines (Fig. 4A). DPP4 secretion increased significantly in Cntrl 1, Cntrl 2, and Stea 1 (0.95±0.11 ng/mL, 0.22±0.04 ng/mL, 2.51±0.27 ng/mL DPP4 under mock conditions and 3.94±0.38 ng/mL, 1.45±0.35 ng/mL, 5.53±0.02 ng/mL, respectively) and not-significantly in Stea 2 (mock: 1.55±0.16 ng/mL, OA: 2.42±0.06 ng/mL).

Interestingly, there was a greater increase of DPP4 secretion upon OA in cell lines derived from healthy individuals, compared to patient derived HLCs. DPP4 levels increased approximately 4.5- to 5-fold in Cntrl 1 and 2 while Stea 1 and 2 showed a DPP4 increase of 2-fold and 0.8-fold, respectively. This probably indicates that the control cell lines are able to increase DPP4 secretion more strongly in response to OA. Moreover, Stea 2 showed the lowest and non-significant increase of DPP4 secretion compared to the others. This might underline differences in the genetic background in comparison to the other cell lines, which we have already detected in the global transcriptome analysis. To gain insights into the mechanisms underlying upregulation of DPP4 upon OA-treatment, we analyzed the gene expression in the four cell lines, however we could not detect a significant change upon OA-induction (Fig. 4B). To elucidate the role of DPP4 in steatosis, we focused for the further analyses on the Cntrl cell lines, because of the stronger induction of DPP4 secretion upon OA. Similar to the

gene expression of *DPP4*, we did not detect a prominent change in the protein localization or amount upon OA (Fig. 4C).

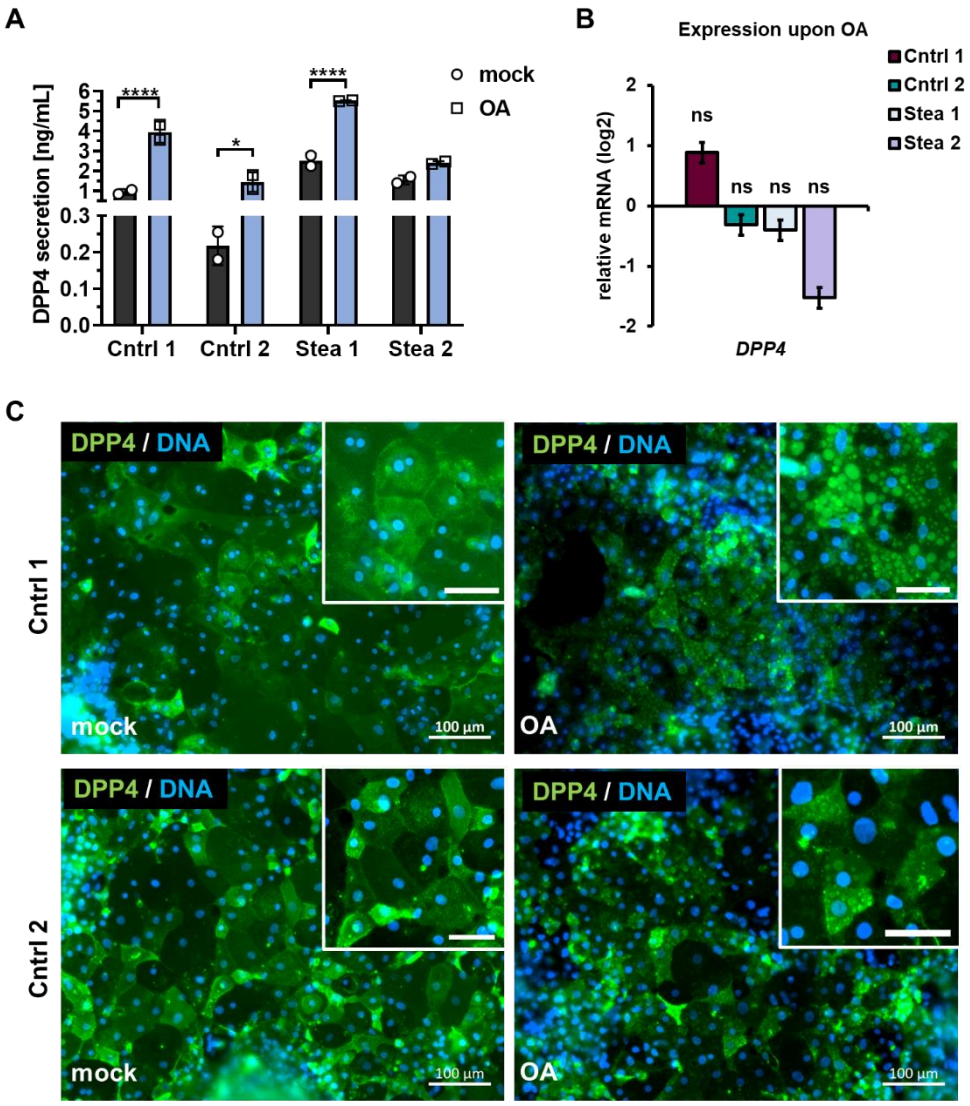

Fig. 4 DPP4 is secreted upon OA-treatment. (A) Secretion of Dipeptidyl peptidase (DPP4) upon OA-treatment measured by ELISA-detection, showing secreted DPP4 as the mean of two biological replicates (n=2 ±SD). Ordinary two-way ANOVA, followed by Sidak's multiple comparison test was performed to calculate significances (*$p < 0.05$, ****$p < 0.0001$). **(B)** Gene expression of *DPP4* upon OA treatment relative to mock treatment in four cell lines, shown are means of three biological replicates, normalized to the housekeeping gene *RPLP0* (n=3 ±SE). Two-tailed unpaired Student`s T-test was performed to calculate significances (ns $p > 0.05$). **(C)** Representative immunocytochemistry of DPP4 under mock and OA conditions in cell lines Cntrl 1 and Cntrl 2. Scale bars represent 100 µm and 50 µm in the zoom-in.

Vildagliptin reduces DPP4 activity

Vildagliptin (VILDA) was tested in a phase-4 study (ID NCT01356381) to elucidate its potential use for treating steatosis patients(33). However, whether VILDA improves the hepatic phenotype directly or by incretin regulation, is yet to be elucidated. To shed light on its direct effects on hepatocytes, we induced the steatosis phenotype in our HLCs by a pre-treatment with OA for 48 h followed by incubation with 30 µM VILDA for a total of 5 days simultaneously with OA. We did not detect significant difference in *DPP4* expression on both the RNA and protein level upon the treatments in comparison to mock w/o VILDA (Fig. 5A-C), while we detected an expectedly strong increase for PLIN2 after OA induction in Cntrl 1 and 2 HLCs (Fig. 5B/C).

Considering the secretion of DPP4, we confirmed the previously detected increase of DPP4 upon OA w and w/o VILDA for both cell lines in comparison to the mock treatment. However, no significant difference upon VILDA treatment was detectable (Fig. 5D). Nevertheless, we detected a significant increase of DPP4 activity for both cell lines upon OA treatment which was significantly reduced when HLCs were treated with OA and VILDA together (Fig. 5 E). VILDA is capable of reducing DPP4 activity to the level detected under mock conditions, with no significant difference between OA w VILDA and mock w/o VILDA. These findings confirm that VILDA mainly acts on DPP4 activity, and neither on its gene or protein expression, nor on its secretion.

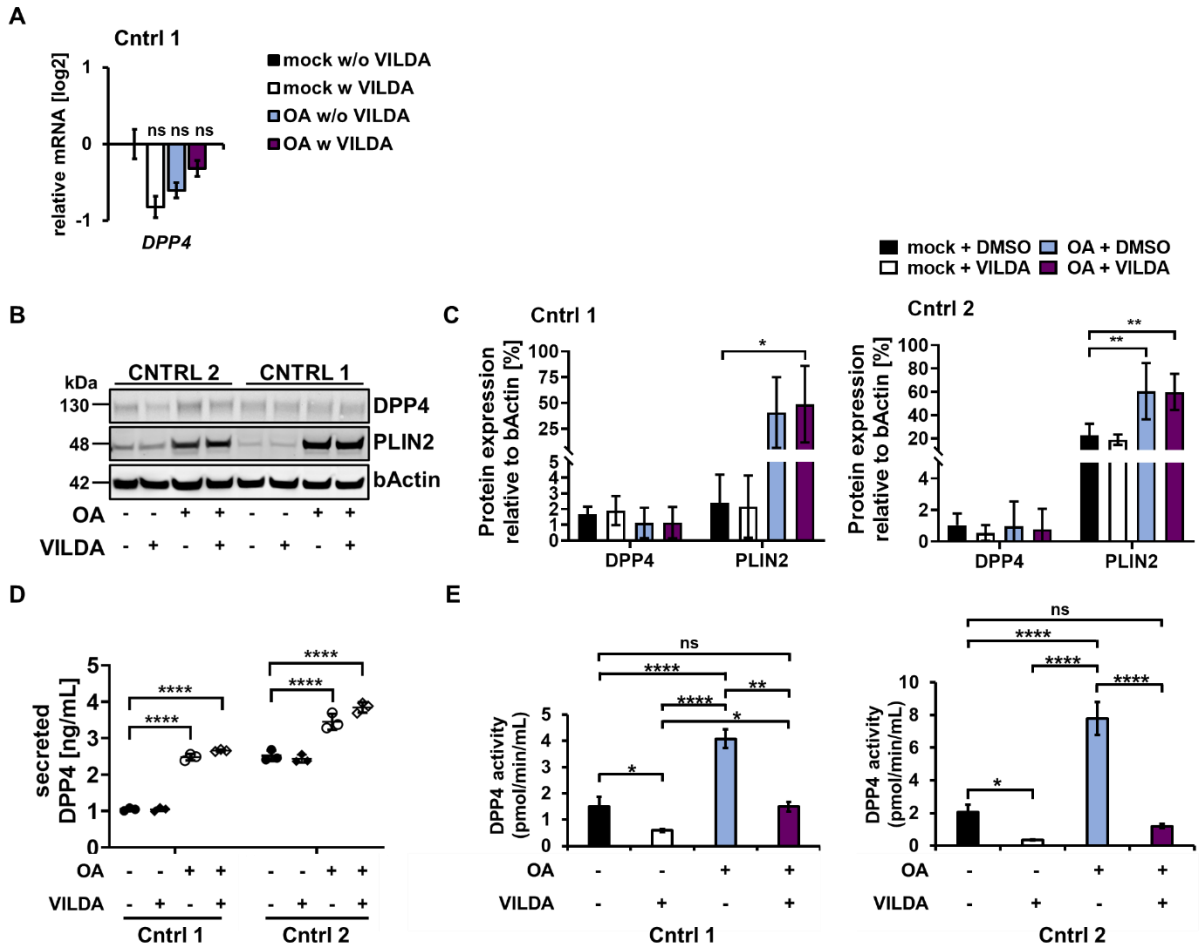

Fig. 5 Effects of Vildagliptin on OA-induced HLCs. (A) Gene expression of *DPP4* in Cntrl 1 HLCs upon OA-treatment with (w) and without (w/o) 30 µM Vildagliptin (VILDA) for 5 days, in comparison to mock w/o VILDA, shown are means of three biological replicates, normalized to the housekeeping gene *RPLP0* (n=3 ±SE). Ordinary one-way ANOVA followed by Tukey's multiple comparisons was performed to calculate significances (ns p> 0.05). **(B)** Representative WB of DPP4 and PLIN2 upon OA-treatment w and w/o VILDA. **(C)** Protein expression relative to bActin in comparison to mock w/o VILDA. Shown are means of three biological replicates (n=3 ± SD). Ordinary two-way ANOVA, followed by Tukey's multiple comparison test was performed to calculate significances (*p < 0.05, **p < 0.01). **(D)** DPP4 secretion upon OA-treatment w and w/o VILDA. Shown are means of three biological replicates (n=3 ±SD). Ordinary two-way ANOVA, followed by Dunnet's multiple comparison test was performed to calculate significances (**p < 0.01, ***p < 0.001, ****p < 0.001). **(E)** DPP4 activity in HLCs upon OA-treatment w and w/o VILDA was analyzed by measuring the proteolytic activity over time. Ordinary one-way ANOVA and Tukey's multiple comparison test was performed to calculate significances (*p < 0.05, ****p < 0.001).

Inhibition of DPP4 activity might reduce inflammatory progression leading to the disease phenotype

To test whether VILDA further affects other genes involved in the steatosis phenotype, we analyzed the global gene expression upon OA w and w/o VILDA in cell line Cntrl 1. First level dendrogram analysis revealed clustering according to mock- and OA-treatment, however not according to the VILDA treatment, indicating a stronger impact of OA on the gene expression in comparison to VILDA (Fig. S5A). To confirm the previously detected gene expression pattern in response to OA, we performed KEGG-associated pathway analysis of the gene expression upon OA w/o VILDA in comparison to mock w/o VILDA (Fig. S5B/C). Indeed, we found similar pathways to be differentially regulated upon OA w/o VILDA in comparison to the previous data, indicating that the solvent reagent had no impact on the OA-response (Fig. S5B/C).

In addition to the 14,118 genes expressed in common in all four conditions, we found exclusively expressed gene sets for every condition as indicated by Venn analysis (Fig. 6A). We found 91 and 339 exclusively expressed genes upon OA w VILDA and mock w VILDA, respectively. 62 and 115 genes were exclusively expressed upon OA w/o VILDA and mock w/o VILDA treatment, respectively. KEGG- and Gene Ontologies (GO)- associated pathway analyses for the exclusively expressed genes upon the different conditions did not reveal characteristic profiles (Table S2), except for an exclusive expression of genes associated to KEGG pathways related to cancer after VILDA treatment (Table S2). In general, our findings underline a rather mild effect of VILDA compared to OA and for further analyses, we included both the exclusively and common but differentially expressed genes.

Next, we wanted to know, whether VILDA influences gene expression upon OA treatment and found 29 genes significantly up- and 31 genes significantly

downregulated upon VILDA treatment (Fig. 6B). KEGG- pathway analysis revealed genes belonging to the inflammatory bowel disease pathway, asthma and type 1 diabetes mellitus (T1DM) associated pathways significantly downregulated (Fig. 6C and Fig. S7A). Common downregulated genes of these pathways encode members of the Human leukocyte antigen II (HLAII) family, namely HLA-DQA1 and HLA-DMB, which are known to be ectopically expressed on hepatocytes upon hepatitis(34-36). Although the expression changes were small, we confirmed upregulation of *HLA-DMA*, *HLA-DMB* and *HLA-DRB1* upon OA-treatment and a tendency towards downregulation upon OA w VILDA (Fig. 6E). This might indicate a potential association between DPP4 and HLAs in steatosis. Interestingly, in contrast to the RNA-seq we found *HLA-DQA1* downregulated upon OA and a slight increase of expression upon OA w VILDA treatment (Fig. 6E).

Genes associated with metabolic pathways, such as purine metabolism and fatty acid biosynthesis pathways were upregulated in OA w VILDA versus OA w/o VILDA (Fig. 6D and Fig. S7A). Interestingly, we found triokinase and FMN cyclase (*TKFC*), and 5'-nucleotidase, cytosolic II (*NT5C2*), both members of the purine metabolism, downregulated upon OA w/o VILDA in comparison to mock w/o VILDA, while VILDA treatment induced an upregulation, which might indicate a restoration of the pathway (Fig. 6F). Considering fatty acid metabolism, we detected O-acyltransferase 2 (*AGPAT2*) upregulated upon OA w/o VILDA treatment in comparison to mock w/o VILDA which was even reinforced upon OA w VILDA (Fig. 6F). We saw the same trend in gene expression of perilipin-3 (*PLIN3*) however, we did not detect differential protein expression (Fig. 6F-G). In contrast, considering another member of the perilipin family, namely PLIN2, we detected the same gene expression pattern, but differential protein expression (Fig. S6B, Fig. 6F). PLIN2 protein levels were

upregulated upon OA, while PLIN3 protein levels were stable throughout the conditions. A reason might be, that PLIN3 belongs to the exchangeable PLINs, while PLIN2 is a constitutive protein, upregulated upon OA-treatment and unstable in the absence of LDs(37). PLIN3 is stable in the cytoplasm independently of LDs but is recruited to the lipid fractions(37). Nevertheless, considering the mRNA expression, our findings might indicate that DPP4 inhibition upon OA restores the hampered cellular energy homeostasis, however further studies are necessary to pinpoint the underlying mechanism.

To test whether VILDA affects the expression of steatosis-associated genes, we evaluated the steatosis gene set from the earlier global analysis. We could confirm the same trend of gene expression for Cntrl 1 upon OA (Fig. S6A), while we could not detect a significant difference when comparing OA w/o and w VILDA for any of the genes. These findings underline the hypothesis that DPP4 inhibition interferes with the gene expression in response to OA, and targets specific pathways such as fatty acid and purine metabolism.

To gain insights into the overall VILDA effect, independent of the steatosis condition, we performed KEGG-pathway analysis of the genes differentially expressed under mock conditions. We found 47 genes significantly upregulated and 44 genes significantly downregulated upon mock w and w/o VILDA treatment (Fig. S8A). KEGG-associated pathway analysis revealed, among others, downregulated genes associated with inflammatory response pathways under mock conditions (Fig. S8B). Upregulated genes were involved in KEGG-associated pathways indicating enhanced metabolism and insulin secretion, indicating beneficial effects for the compromised insulin pathway, since insulin resistance pathway was upregulated upon OA (Fig. S8C). Altogether, our findings strengthen the hypothesis that DPP4 is involved not only in

metabolic regulation via purine and fatty acid metabolism but furthermore affects inflammatory response, possibly via interference with the HLA class II proteins in hepatocytes.

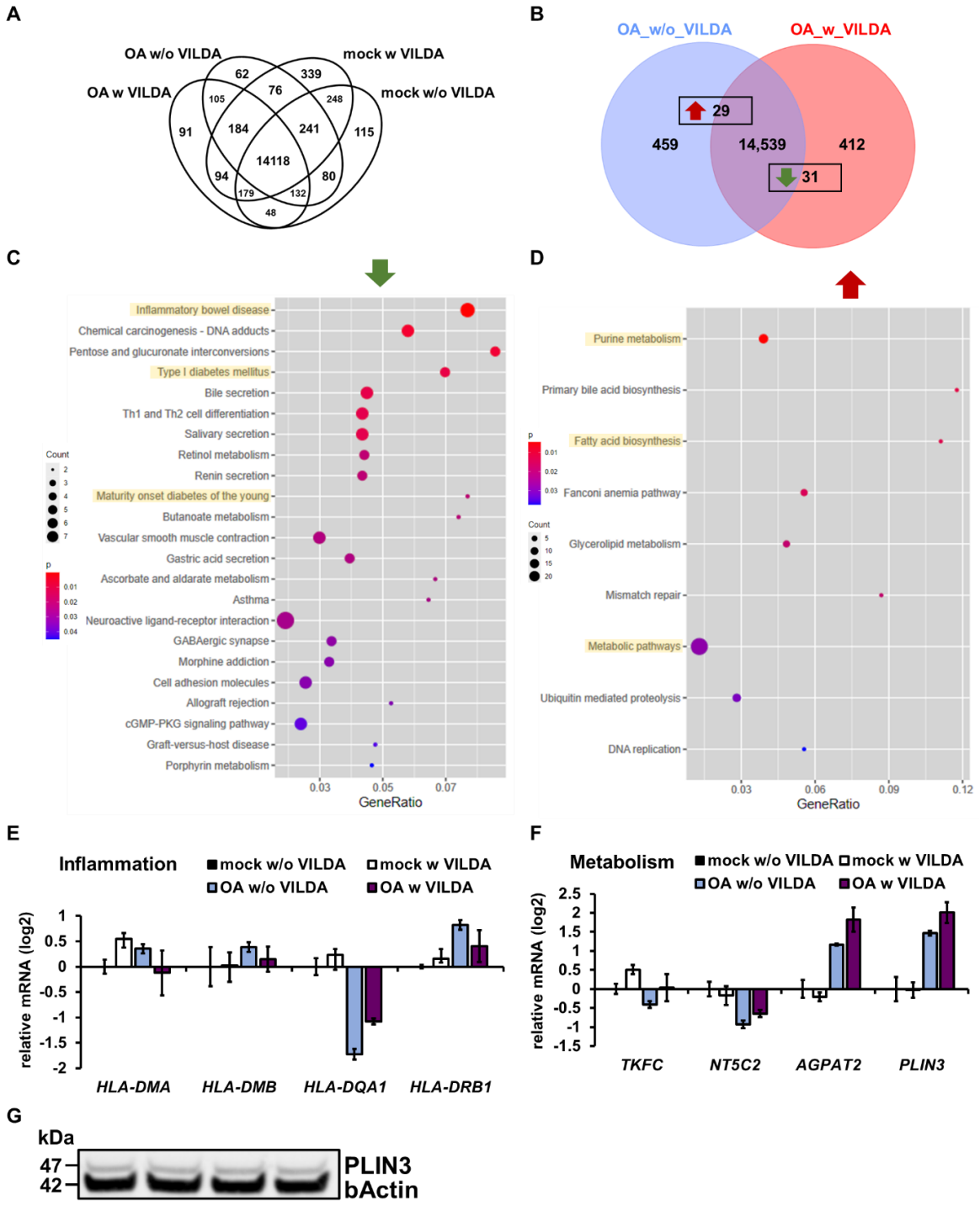

Fig. 6 VILDA effects on the global transcription of steatotic Ctrl1 HLCs. (A) Venn diagram of expressed genes upon indicated treatments. **(B)** Venn diagram of the gene expression of OA treated HLCs w and w/o VILDA. **(C,D)** KEGG-associated pathways of significantly down-

(C) and up- **(D)** regulated genes upon OA w VILDA treatment. **(E,F)** Gene expression of inflammation-associated **(E)** and metabolism-associated **(F)** genes upon OA w and w/o VILDA treatment. **(G)** Western blot analysis of Perilipin-3 (PLIN3) upon OA w and w/o VILDA in comparison to housekeeping protein b-Actin.

Discussion:

Oleic acid feeding induces clinically relevant phenotype of steatosis

In this study, we generated induced pluripotent stem cell (iPSC)- derived steatotic hepatocyte-like cells (HLCs) from four individuals to elucidate the potential hepatocyte-specific contribution to the progression of MAFLD. HLCs expressed typical hepatocyte markers and showed CYP-activity. By stimulating HLCs with OA, we were able to induce lipid droplet formation in all four cell lines, as already shown in previous studies(7, 8). Interestingly, we found cell line-specific differences in the amount and size of the lipid droplets. This is in line with our previously published data and the high divergence in individual symptoms and progression of MAFLD which are well-known difficulties in the clinic(7). They are due to genetic variations like single nucleotide polymorphisms (SNPs), epigenetic alterations and other co-morbidities that are associated with the disease(38, 39). Furthermore, considerable variability is typical for iPSC-derived data due to the individual genetic background and differences in differentiation efficiencies. Indeed, we excluded the patient derived cell line Stea 2 due to ambiguous clustering in the first level analysis.

Global transcriptomic analyses revealed MAFLD-associated pathways such as metabolism-associated and immune-modulating pathways differentially regulated in our model(40-42). A heatmap analysis of genes from these pathways, revealed clustering according to the treatment and independent of the genetic background. This underlines the importance of the involved genes for the disease. Although our model comprises only hepatocytes, the detected upregulation of cytokine-cytokine receptor

signaling, NF-kappa B and TNF signaling upon OA might indicate immune cell recruitment via inflammatory/ chemokine signaling. Recently, Yu et al demonstrated that hepatocyte-intrinsic changes contribute to the disease(41) while predisposition, environment, or other comorbidities might further regulate the pace of the progression towards fibrosis and cirrhosis. Comparing the gene expression profile detected in our HLCs with their single cell RNA-seq data from liver resections of NASH and HCC-patients, we found many pathways upregulated that are associated with a lower risk of NASH-HCC-transition, such as galactose catabolic processes, hexose metabolic processes, and glucose homeostasis.

Active Dipeptidyl peptidase 4 (DPP4) is secreted upon OA treatment

DPP4 is a serine protease with catalytic activity for various substrates(12) and considered a hepatokine, upregulated in metabolic liver disease and driver of inflammation(13). Similar to observations made in HepG2 cells(43), we could not detect elevated DPP4 on both the mRNA or protein level. However, we found elevated secretion and a drastic increase in the catalytic activity of DPP4 upon OA, in line with previously observed elevation in NAFLD/NASH patients(44, 45). As DPP4 is involved in various chronic and cancerous diseases throughout the human body, hepatocyte-specific secretion upon late-steatosis might indicate inflammatory signaling and a risk for the development of other comorbidities like cardiovascular and renal diseases(46).

VILDA interferes with DPP4 activity and regulates inflammatory and metabolism associated gene expression

To elucidate the mechanism of action of DPP4, we inhibited its activity with VILDA- an FDA-approved T2DM medication. As a proof-of-principle, we found that VILDA interferes solely with DPP4 activity and not with the protein or mRNA level, as described in previous studies(47). Global transcriptome analysis revealed clustering

according to the OA- /mock treatment, but not according to the VILDA treatment. This confirmed our expectation that OA treatment induced greater transcriptome changes than VILDA treatment. Nevertheless, we detected exclusively expressed genes for all four conditions. Although KEGG-associated pathway analysis did not identify characteristic profiles, we noticed that genes involved in the development of cancer were upregulated upon VILDA independently of steatosis. VILDA-associated safety concerns have already been extensively addressed and no significant overall cancer-association was found(48, 49). Considering the typical long-term or even life-long medication of T2DM, this should nevertheless be monitored carefully.

Furthermore, we found inflammation associated pathways such as Type 1 diabetes mellitus (T1DM), inflammatory bowel disease and asthma downregulated upon DPP4 inhibition. *HLA-DQA1* and *HLA-DMB* are common genes involved in all of them, and their expression was differentially regulated upon steatosis and additional DPP4 inhibition. HLA class II proteins are typically expressed on the surface of antigen presenting cells, however ectopic expression in hepatocytes upon disease has been shown(34, 36). In line with this, we found elevated gene expression of *HLA-DMB*, *HLA-DMA* and *HLA-DRB1* upon OA, which are associated with NASH, hepatitis and cirrhosis(50, 51), and all decreased upon DPP4 inhibition. Since DPP4 activity apparently affects the expression of genes involved in (auto)-immune related diseases, this might provide a possible clue towards its role for inflammation.

To understand the role of DPP4 for the interplay between metabolism and inflammation, it is essential to determine, whether DPP4 is causal or correlative for late-steatosis. DPP4 was shown to be epigenetically regulated(52, 53). Indeed, we also found a slight albeit not significant demethylation upon OA treatment (not shown). This supports the speculation that early events of energy overload might change the methylation profiles

of CpG islands in the DPP4 locus and enable DPP4 expression in hepatocytes at a rather early timepoint of disease progression.

The insulin resistance pathway was upregulated upon OA treatment, which matches with the well-known insulin resistance promoting effect of DPP4(54). Interestingly, we found genes involved in purine and fatty acid metabolism upregulated upon VILDA treatment. E.g. *AGPAT2,* which is involved in fatty acid metabolism, was upregulated upon DPP4 inhibition. Its deletion or mutation is associated with insulin resistance, diabetes and severe forms of metabolic syndrome in mice and humans(55-57). This could indicate a VILDA-mediated beneficial effect for the hampered metabolism due the energy overload during late-steatosis and underline the idea of a role for DPP4 in the interplay between metabolism and inflammation(15, 54).

Conclusions:

Taken together, we provide a human iPSC-derived model focusing on the hepatocyte-specific contribution to progression of steatosis. We could link DPP4 activity to the steatosis phenotype and show that its inhibition with Vildagliptin has beneficial effects on metabolism and inflammation during steatosis. In the future, human DPP4-knockout HLCs, embedded in a multicellular liver model, could increase our understanding of the mechanisms of DPP4 through health and disease and help to further elucidate the interplay between the distinct cell types of the liver.

Abbreviations:

ACE2	Angiotensin converting enzyme 2
AFP	Alpha-Fetoprotein
AGPAT2	O-acyltransferase 2
ALB	Albumin
AMPK	Adenosine monophosphate-activated protein kinase
ANPEP	Alanyl Aminopeptidase
CCL4	C-C motif chemokine ligand 4

CD26	Cluster of differentiation 26
Cntrl	Control
CPT1A	Carnitine palmitoyltransferase I
CYP	Cytochrome P450
DE	Definitive endoderm
Dex	Dexamethasone
DPP4	Dipeptidyl peptidase 4
E-CAD	E Cadherin
ELISA	Enzyme-linked immunosorbent assay
FABP1	fatty acid binding protein 1
FDA	Food and drug administration (U.S.)
GOs	Gene ontologies
GSK-3	Glycogen synthase kinase 3
HE	Hepatic endoderm
HGF	Hepatocyte growth factor
HLAII	Human leukocyte antigen II
HLCs	Hepatocyte like cells
HNF4a	Hepatocyte nuclear factor 4alpha
IGFBP1	Insulin Like Growth Factor Binding Protein 1
igG	Immunoglobulin G
IL1B	Interleukin 1beta
iPSCs	induced pluripotent stem cells
KEGG	Kyoto Encyclopedia of Genes and Genomes
LD	Lipid droplet
MAFLD	Metabolic dysfunction-associated fatty liver disease
MASLD	Metabolic dysfunction-associated steatotic liver disease
NAFLD	Non-alcoholic fatty liver disease
NASH	Non-alcoholic steatohepatitis
NT5C2	5'-nucleotidase, cytosolic II
OA	Oleic acid
OCT4	octamer-binding transcription factor 4
OSM	Oncostatin M
P/S	Penicillin/Streptomycin
PCK1	Phosphoenolpyruvate Carboxykinase 1
PLIN2	Perilipin-2
PLIN3	Perilipin-3
PPAR	Peroxisome proliferator activated-receptor
qRT-PCR	Quantitative reverse transcription PCR
R.L.U.	Relative light units
RNA-seq	RNA sequencing
ROS	Reactive oxygen species
RPLP0	Ribosomal Protein Lateral Stalk Subunit P0
SNPs	single nucleotide polymorphisms
SOX	SRY-related HMG-box genes

Stea	Steatosis
T1DM	Type 1 diabetes mellitus
T2DM	Type 2 diabetes mellitus
TBS-T	Tris-buffered saline with Tween20
TKFC	Triokinase and FMN cyclase
TNF	Tumor necrosis factor
VCAM1	Vascular cell adhesion molecule 1
VILDA	Vildagliptin

Data availability statement:

The data that support the findings of this study are available from the corresponding author upon reasonable request.

Acknowledgments:

C.L., N.G. and J.R. are funded by the Else Kröner-Fresenius-Stiftung – 2020_EKEA.64. J.A. acknowledges the medical faculty of Heinrich-Heine University Düsseldorf for part funding of this project.

1. Angulo P. Obesity and nonalcoholic fatty liver disease. Nutr Rev 2007;65:S57-63.
2. Eslam M, Newsome PN, Sarin SK, Anstee QM, Targher G, Romero-Gomez M, Zelber-Sagi S, et al. A new definition for metabolic dysfunction-associated fatty liver disease: An international expert consensus statement. J Hepatol 2020;73:202-209.
3. Henry L, Paik J, Younossi ZM. Review article: the epidemiologic burden of non-alcoholic fatty liver disease across the world. Aliment Pharmacol Ther 2022;56:942-956.
4. Teng ML, Ng CH, Huang DQ, Chan KE, Tan DJ, Lim WH, Yang JD, et al. Global incidence and prevalence of nonalcoholic fatty liver disease. Clin Mol Hepatol 2023;29:S32-s42.
5. Barrera F, Uribe J, Olvares N, Huerta P, Cabrera D, Romero-Gómez M. The Janus of a disease: Diabetes and metabolic dysfunction-associated fatty liver disease. Ann Hepatol 2024;29:101501.
6. Zhao J, Liu L, Cao YY, Gao X, Targher G, Byrne CD, Sun DQ, et al. MAFLD as part of systemic metabolic dysregulation. Hepatol Int 2024.
7. Graffmann N, Ncube A, Martins S, Fiszl AR, Reuther P, Bohndorf M, Wruck W, et al. A stem cell based in vitro model of NAFLD enables the analysis of patient specific individual metabolic adaptations in response to a high fat diet and AdipoRon interference. Biol Open 2021;10.
8. Graffmann N, Ring S, Kawala MA, Wruck W, Ncube A, Trompeter HI, Adjaye J. Modeling Nonalcoholic Fatty Liver Disease with Human Pluripotent Stem Cell-Derived Immature Hepatocyte-Like Cells Reveals Activation of PLIN2 and Confirms Regulatory Functions of Peroxisome Proliferator-Activated Receptor Alpha. Stem Cells Dev 2016;25:1119-1133.

616 9. Wruck W, Kashofer K, Rehman S, Daskalaki A, Berg D, Gralka E, Jozefczuk J, et al. Multi-omic
617 profiles of human non-alcoholic fatty liver disease tissue highlight heterogenic phenotypes. Sci Data
618 2015;2:150068.
619 10. Beygi M, Ahi S, Zolghadri S, Stanek A. Management of Metabolic-Associated Fatty Liver
620 Disease/Metabolic Dysfunction-Associated Steatotic Liver Disease: From Medication Therapy to
621 Nutritional Interventions. Nutrients 2024;16.
622 11. Lara-Romero C, Romero-Gómez M. Treatment Options and Continuity of Care in Metabolic-
623 associated Fatty Liver Disease: A Multidisciplinary Approach. Eur Cardiol 2024;19:e06.
624 12. Mulvihill EE, Drucker DJ. Pharmacology, physiology, and mechanisms of action of dipeptidyl
625 peptidase-4 inhibitors. Endocr Rev 2014;35:992-1019.
626 13. Trzaskalski NA, Fadzeyeva E, Mulvihill EE. Dipeptidyl Peptidase-4 at the Interface Between
627 Inflammation and Metabolism. Clin Med Insights Endocrinol Diabetes 2020;13:1179551420912972.
628 14. Ahrén B, Landin-Olsson M, Jansson PA, Svensson M, Holmes D, Schweizer A. Inhibition of
629 dipeptidyl peptidase-4 reduces glycemia, sustains insulin levels, and reduces glucagon levels in type 2
630 diabetes. J Clin Endocrinol Metab 2004;89:2078-2084.
631 15. Ghorpade DS, Ozcan L, Zheng Z, Nicoloro SM, Shen Y, Chen E, Bluher M, et al. Hepatocyte-
632 secreted DPP4 in obesity promotes adipose inflammation and insulin resistance. Nature
633 2018;555:673-677.
634 16. Ohm B, Moneke I, Jungraithmayr W. Targeting cluster of differentiation 26 / dipeptidyl
635 peptidase 4 (CD26/DPP4) in organ fibrosis. Br J Pharmacol 2023;180:2846-2861.
636 17. Hussain M, Majeed Babar MZ, Hussain MS, Akhtar L. Vildagliptin ameliorates biochemical,
637 metabolic and fatty changes associated with non alcoholic fatty liver disease. Pak J Med Sci
638 2016;32:1396-1401.
639 18. Hendawy AS, El-Lakkany NM, Mantawy EM, Hammam OA, Botros SS, El-Demerdash E.
640 Vildagliptin alleviates liver fibrosis in NASH diabetic rats via modulation of insulin resistance,
641 oxidative stress, and inflammatory cascades. Life Sci 2022;304:120695.
642 19. Khalil R, Shata A, Abd El-Kader EM, Sharaf H, Abdo WS, Amin NA, Saber S. Vildagliptin, a DPP-
643 4 inhibitor, attenuates carbon tetrachloride-induced liver fibrosis by targeting ERK1/2, p38alpha, and
644 NF-kappaB signaling. Toxicol Appl Pharmacol 2020;407:115246.
645 20. Loerch C, Szepanowski L-P, Reiss J, Adjaye J, Graffmann N. Forskolin induces FXR expression
646 and enhances maturation of iPSC-derived hepatocyte-like cells. Frontiers in Cell and Developmental
647 Biology 2024;12.
648 21. Bohndorf M, Ncube A, Spitzhorn LS, Enczmann J, Wruck W, Adjaye J. Derivation and
649 characterization of integration-free iPSC line ISRM-UM51 derived from SIX2-positive renal cells
650 isolated from urine of an African male expressing the CYP2D6 *4/*17 variant which confers
651 intermediate drug metabolizing activity. Stem Cell Res 2017;25:18-21.
652 22. Kawala MA, Bohndorf M, Graffmann N, Wruck W, Zatloukal K, Adjaye J. Characterization of
653 iPSCs derived from dermal fibroblasts from a healthy 19year old female. Stem Cell Res 2016;17:597-
654 599.
655 23. Kawala MA, Bohndorf M, Graffmann N, Wruck W, Zatloukal K, Adjaye J. Characterization of
656 dermal fibroblast-derived iPSCs from a patient with high grade steatosis. Stem Cell Res 2016;17:568-
657 571.
658 24. Graffmann N, Bohndorf M, Ncube A, Wruck W, Kashofer K, Zatloukal K, Adjaye J.
659 Establishment and characterization of an iPSC line from a 58 years old high grade patient with
660 nonalcoholic fatty liver disease (70% steatosis) with homozygous wildtype PNPLA3 genotype. Stem
661 Cell Res 2018;31:131-134.
662 25. Kim D, Langmead B, Salzberg SL. HISAT: a fast spliced aligner with low memory requirements.
663 Nat Methods 2015;12:357-360.
664 26. Kanehisa M, Furumichi M, Tanabe M, Sato Y, Morishima K. KEGG: new perspectives on
665 genomes, pathways, diseases and drugs. Nucleic Acids Res 2017;45:D353-d361.
666 27. Falcon S, Gentleman R. Using GOstats to test gene lists for GO term association.
667 Bioinformatics 2007;23:257-258.

668 28. Wickham H. ggplot2: Springer New York, NY, 2009.
669 29. Schneider CA, Rasband WS, Eliceiri KW. NIH Image to ImageJ: 25 years of image analysis. Nat
670 Methods 2012;9:671-675.
671 30. Gentleman RC, Carey VJ, Bates DM, Bolstad B, Dettling M, Dudoit S, Ellis B, et al.
672 Bioconductor: open software development for computational biology and bioinformatics. Genome
673 Biol 2004;5:R80.
674 31. Wruck W, Boima V, Erichsen L, Thimm C, Koranteng T, Kwakyi E, Antwi S, et al. Urine-Based
675 Detection of Biomarkers Indicative of Chronic Kidney Disease in a Patient Cohort from Ghana. J Pers
676 Med 2022;13.
677 32. Warnes GR, Ben Bolker, Lodewijk Bonebakker, Robert Gentleman, Wolfgang Huber Andy
678 Liaw, Thomas Lumley, Martin Maechler, et al. Gplots: Various R Programming Tools for Plotting Data.
679 In; 2015.
680 33. Macauley M, Hollingsworth KG, Smith FE, Thelwall PE, Al-Mrabeh A, Schweizer A, Foley JE, et
681 al. Effect of vildagliptin on hepatic steatosis. J Clin Endocrinol Metab 2015;100:1578-1585.
682 34. Lu JG, Ji P, French SW. The Major Histocompatibility Complex Class II–CD4 Immunologic
683 Synapse in Alcoholic Hepatitis and Autoimmune Liver Pathology: The Role of Aberrant Major
684 Histocompatibility Complex Class II in Hepatocytes. The American Journal of Pathology 2020;190:25-
685 32.
686 35. Lu JG, Iyasu A, French B, Tillman B, French SW. Overexpression of MHCII by hepatocytes in
687 alcoholic hepatitis (AH) compared to non-alcoholic steatohepatitis (NASH) and normal controls.
688 Alcohol 2020;84:27-32.
689 36. Dezhbord M, Kim SH, Park S, Lee DR, Kim N, Won J, Lee AR, et al. Novel role of MHC class II
690 transactivator in hepatitis B virus replication and viral counteraction. Clin Mol Hepatol 2024;30:539-
691 560.
692 37. Wolins NE, Brasaemle DL, Bickel PE. A proposed model of fat packaging by exchangeable lipid
693 droplet proteins. FEBS Lett 2006;580:5484-5491.
694 38. Metwally M, Eslam M, George J. Genetic and Epigenetic Associations of NAFLD: Focus on
695 Clinical Decision Making. Current Hepatology Reports 2017;16:335-345.
696 39. Tilson SG, Morell CM, Lenaerts AS, Park SB, Hu Z, Jenkins B, Koulman A, et al. Modeling
697 PNPLA3-Associated NAFLD Using Human-Induced Pluripotent Stem Cells. Hepatology 2021;74:2998-
698 3017.
699 40. Wruck W, Graffmann N, Kawala MA, Adjaye J. Concise Review: Current Status and Future
700 Directions on Research Related to Nonalcoholic Fatty Liver Disease. Stem Cells 2017;35:89-96.
701 41. Yu Q, Zhang Y, Ni J, Shen Y, Hu W. Identification and analysis of significant genes in
702 nonalcoholic steatohepatitis-hepatocellular carcinoma transformation: Bioinformatics analysis and
703 machine learning approach. Molecular Immunology 2024;174:18-31.
704 42. Xiong Y, Shi X, Xiong X, Li S, Zhao H, Song H, Wang J, et al. A systematic review and meta-
705 analysis of randomized controlled trials: effects of mediterranean diet and low-fat diet on liver
706 enzymes and liver fat content of NAFLD. Food Funct 2024;15:8248-8257.
707 43. Miyazaki M, Kato M, Tanaka K, Tanaka M, Kohjima M, Nakamura K, Enjoji M, et al. Increased
708 hepatic expression of dipeptidyl peptidase-4 in non-alcoholic fatty liver disease and its association
709 with insulin resistance and glucose metabolism. Mol Med Rep 2012;5:729-733.
710 44. Barchetta I, Ceccarelli V, Cimini FA, Barone E, Sentinelli F, Coluzzi M, Chiappetta C, et al.
711 Circulating dipeptidyl peptidase-4 is independently associated with the presence and severity of
712 NAFLD/NASH in individuals with and without obesity and metabolic disease. J Endocrinol Invest
713 2021;44:979-988.
714 45. Barchetta I, Cimini FA, Dule S, Cavallo MG. Dipeptidyl Peptidase 4 (DPP4) as A Novel
715 Adipokine: Role in Metabolism and Fat Homeostasis. Biomedicines 2022;10:2306.
716 46. Tomovic K, Lazarevic J, Kocic G, Deljanin-Ilic M, Anderluh M, Smelcerovic A. Mechanisms and
717 pathways of anti-inflammatory activity of DPP-4 inhibitors in cardiovascular and renal protection.
718 Med Res Rev 2019;39:404-422.

47. Mathieu C, Degrande E. Vildagliptin: a new oral treatment for type 2 diabetes mellitus. Vasc Health Risk Manag 2008;4:1349-1360.
48. Zhao M, Chen J, Yuan Y, Zou Z, Lai X, Rahmani DM, Wang F, et al. Dipeptidyl peptidase-4 inhibitors and cancer risk in patients with type 2 diabetes: a meta-analysis of randomized clinical trials. Sci Rep 2017;7:8273.
49. Kanazawa I, Tanaka KI, Notsu M, Tanaka S, Kiyohara N, Koike S, Yamane Y, et al. Long-term efficacy and safety of vildagliptin add-on therapy in type 2 diabetes mellitus with insulin treatment. Diabetes Res Clin Pract 2017;123:9-17.
50. Zhang J-j, Shen Y, Chen X-y, Jiang M-l, Yuan F-h, Xie S-l, Zhang J, et al. Integrative network-based analysis on multiple Gene Expression Omnibus datasets identifies novel immune molecular markers implicated in non-alcoholic steatohepatitis. Frontiers in Endocrinology 2023;14.
51. Lu YY, Chen QL, Guan Y, Guo ZZ, Zhang H, Zhang W, Hu YY, et al. Transcriptional profiling and co-expression network analysis identifies potential biomarkers to differentiate chronic hepatitis B and the caused cirrhosis. Mol Biosyst 2014;10:1117-1125.
52. Hyun J, Jung Y. DNA Methylation in Nonalcoholic Fatty Liver Disease. Int J Mol Sci 2020;21.
53. Saussenthaler S, Ouni M, Baumeier C, Schwerbel K, Gottmann P, Christmann S, Laeger T, et al. Epigenetic regulation of hepatic Dpp4 expression in response to dietary protein. J Nutr Biochem 2019;63:109-116.
54. Baumeier C, Schluter L, Saussenthaler S, Laeger T, Rodiger M, Alaze SA, Fritsche L, et al. Elevated hepatic DPP4 activity promotes insulin resistance and non-alcoholic fatty liver disease. Mol Metab 2017;6:1254-1263.
55. Cortés VA, Curtis DE, Sukumaran S, Shao X, Parameswara V, Rashid S, Smith AR, et al. Molecular mechanisms of hepatic steatosis and insulin resistance in the AGPAT2-deficient mouse model of congenital generalized lipodystrophy. Cell Metab 2009;9:165-176.
56. Araújo-Vilar D, Santini F. Diagnosis and treatment of lipodystrophy: a step-by-step approach. J Endocrinol Invest 2019;42:61-73.
57. Agarwal AK, Tunison K, Horton JD, Garg A. Regulated regeneration of adipose tissue in lipodystrophic Agpat2-null mice partially ameliorates hepatic steatosis. iScience 2024;27:109517.
58. Garcia-Macia M, Santos-Ledo A, Leslie J, Paish HL, Collins AL, Scott RS, Watson A, et al. A Mammalian Target of Rapamycin-Perilipin 3 (mTORC1-Plin3) Pathway is essential to Activate Lipophagy and Protects Against Hepatosteatosis. Hepatology 2021;74:3441-3459.